processes

MDPI

Article

Indolyl-Derived 4*H*-Imidazoles: PASE Synthesis, Molecular Docking and In Vitro Cytotoxicity Assay

Egor A. Nikiforov [1], Nailya F. Vaskina [1], Timofey D. Moseev [1], Mikhail V. Varaksin [1,2,*], Ilya I. Butorin [1], Vsevolod V. Melekhin [1,3], Maria D. Tokhtueva [1], Dmitrii G. Mazhukin [4], Alexsei Y. Tikhonov [4], Valery N. Charushin [1,2] and Oleg N. Chupakhin [1,2]

[1] Institute of Chemical Engineering, Ural Federal University, 19 Mira Street, 620002 Ekaterinburg, Russia; e.a.nikiforov@urfu.ru (E.A.N.); nailia.vaskina@urfu.ru (N.F.V.); timofey.moseev@urfu.ru (T.D.M.); iibutorin@urfu.ru (I.I.B.); v.v.melekhin@urfu.ru (V.V.M.); maria.tokhtueva@urfu.ru (M.D.T.); charushin@ios.uran.ru (V.N.C.); chupakhin@ios.uran.ru (O.N.C.)
[2] I.Ya. Postovsky Institute of Organic Synthesis, Ural Branch of the Russian Academy of Sciences, 22 S. Kovalevskoy Street, 620990 Ekaterinburg, Russia
[3] Department of Medical Biology and Genetics, Ural State Medical University, 3 Repina Street, 620028 Ekaterinburg, Russia
[4] N.N. Vorozhtsov Novosibirsk Institute of Organic Chemistry, Siberian Branch of the Russian Academy of Sciences, 9 Akad. Lavrentyev Avenue, 630090 Novosibirsk, Russia; dimok@nioch.nsc.ru (D.G.M.); alyatikh@nioch.nsc.ru (A.Y.T.)
* Correspondence: m.v.varaksin@urfu.ru

Abstract: The strategy of the nucleophilic substitution of hydrogen (S_N^H) was first applied for the metal-free C-H/C-H coupling reactions of 4*H*-imidazole 3-oxides with indoles. As a result, a series of novel bifunctional azaheterocyclic derivatives were obtained in yields up to 95%. In silico experiments on the molecular docking were performed to evaluate the binding possibility of the synthesized small azaheterocyclic molecules to the selected biotargets (BACE1, BChE, CK1δ, AChE) associated with the pathogenesis of neurodegenerative diseases. To assess the cytotoxicity for the synthesized compounds, a series of in vitro experiments were also carried out on healthy human embryo kidney cells (HEK-293). The leading compound bearing both 5-phenyl-4*H*-imidazole and 1-methyl-1*H*-indole moieties was defined as the prospective molecule possessing the lowest cytotoxicity (IC_{50} > 300 μM on HEK-293) and the highest binding energy in the protein–ligand complex (AChE, −13.57 kcal/mol). The developed compounds could be of particular interest in medicinal chemistry, particularly in the targeted design of small-molecule candidates for the treatment of neurodegenerative disorders.

Keywords: azaheterocycles; indoles; imidazoles; C-H functionalization; nucleophilic substitution of hydrogen; PASE; in vitro cytotoxicity assay; neurodegenerative diseases; molecular docking

Citation: Nikiforov, E.A.; Vaskina, N.F.; Moseev, T.D.; Varaksin, M.V.; Butorin, I.I.; Melekhin, V.V.; Tokhtueva, M.D.; Mazhukin, D.G.; Tikhonov, A.Y.; Charushin, V.N.; et al. Indolyl-Derived 4*H*-Imidazoles: PASE Synthesis, Molecular Docking and In Vitro Cytotoxicity Assay. *Processes* **2023**, *11*, 846. https://doi.org/10.3390/pr11030846

Academic Editor: Liangliang Song

Received: 15 February 2023
Revised: 4 March 2023
Accepted: 7 March 2023
Published: 12 March 2023

1. Introduction

Nowadays, as life expectancy increases, the number of people being affected by neurodegenerative diseases is steadily growing as well. Such pathologies include Alzheimer's disease (AD), which is characterized by latent onset and the gradual progression of loss [1]; Parkinson's disease (PD), which leads to impaired functioning of the musculoskeletal system [2]; frontotemporal dementia/amyotrophic lateral sclerosis (FTD/ALS), which is characterized by the relentless progression of skeletal muscle weakness [3]; and Huntington's disease (HD), which leads to a progressive motor disorder and cognitive disturbance culminating in dementia and psychiatric disturbances [4].

There are several approaches in modern medical practice for the treatment of neurodegenerative pathologies. One of them is the prevention of mitochondrial dysfunction, which directly affects the pathogenesis of neurodegenerative diseases [5]. The next means of therapy is the inhibition of acetylcholine (AChE) and butyrylcholine esterases (BChE), which promote the progression of AD by rapidly hydrolyzing acetylcholine (ACh), which

results in the termination of signaling at the cholinergic synaptic cleft [6]. Another approach is the inhibition of casein kinase 1δ (CK1δ), a serine/threonine-selective enzyme that is responsible for the regulation of signaling pathways in most types of eukaryotic cells [7]. Additionally, the inhibition of beta-secretase-1 (BACE1) prevents the formation of amyloid plaques, which are one of the main causes of the progression of Alzheimer's disease [8]. Therefore, the development of compounds as inhibitors of enzymes that have an impact on the progression of neurodegenerative diseases is one of the key multidisciplinary tasks for modern organic synthesis and medicinal chemistry.

It is well known that small molecules containing imidazole scaffolds have a wide range of biological activities, including neuroprotective ones (Figure 1) [9]. For example, compound **I** is an inhibitor of AChE, and imidazole-containing molecule **II** is an inhibitor of the Monoamine Oxidase-B (MAOB) associated with Parkinson's disease progression [6,10]. Meanwhile, compound **III** is an inhibitor of cyclooxygenase (COX), which directly affects the progression of neurodegenerative diseases [11]. Imidazole derivatives modified by azaheterocyclic fragments, particularly indole scaffolds, form a special class of bicyclic compounds with various biological and pharmacological activities (antibacterial, antidepressant, antioxidant, etc.) [12]. For instance, compound **IV** is a protein kinase C inhibitor, which is one of the targets for the treatment of AD [13], while the imidazole derivative **V** is of interest as an effective 5-HT_7 serotonin receptor agonist [14]. Thus, the development of novel synthetic methodologies to obtain indolyl imidazole is a challenging task in the design of new drug candidates for the therapy of neurodegenerative diseases.

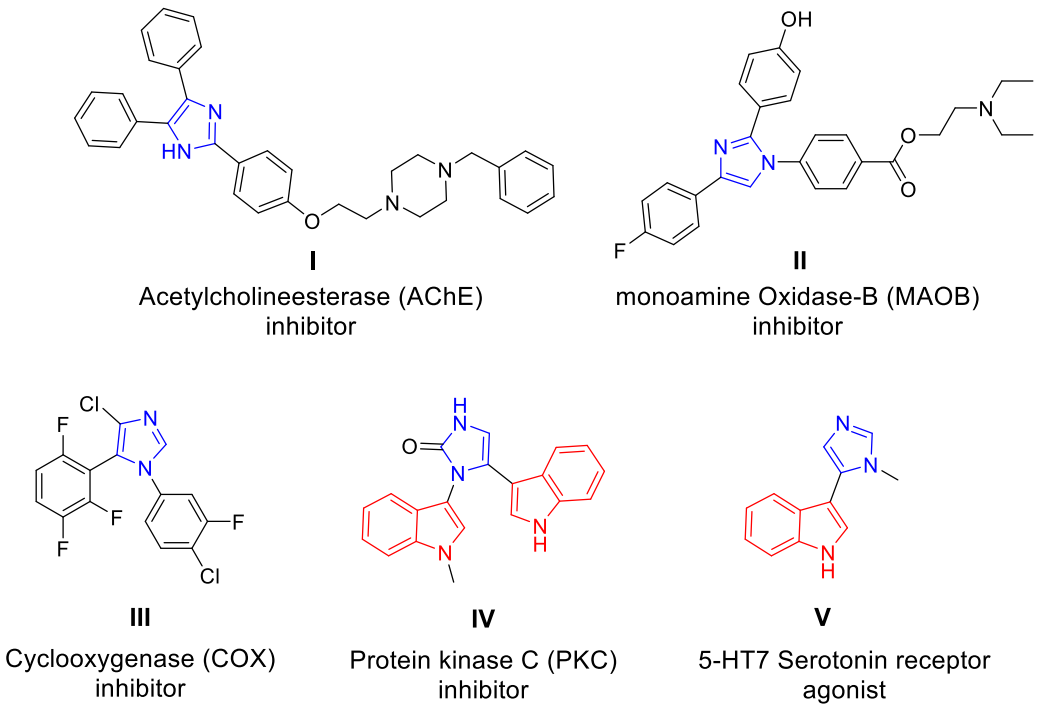

Figure 1. Active pharmaceutical ingredients (APIs) based on imidazole or indolyl-derived imidazole scaffolds (Blue color indicates the imidazole ring, red color shows the indole moiety).

There have been a number of synthetic strategies to design indolyl-derived imidazole compounds. For example, these promising molecular systems can be synthesized by constructing indole or imidazole cycles (Scheme 1a) [15–21]. Besides this, it is possible to use direct coupling between these substrates for the synthesis of the desired compounds [22–25]. Moreover, both transitional-metal-catalyzed and metal-free couplings of imidazole and indole are also utilized (Scheme 1b). For instance, our research group previously reported C-H/C-H coupling of 2*H*-imidazole-1-oxides with indoles [26] (Scheme 1c). It is worth mentioning that these processes were carried out following the Pot, Atom and Step Econom-

ical (PASE) and green chemistry principles [27–29] (e.g., using non-toxic solvents, reducing the number of by-products, etc.) One of the most progressive synthetic methodologies that supports these principles is the C-H functionalization strategy. Subsequently, reactions of the nucleophilic substitution of hydrogen (S_N^H) are considered as special cases of chemical transformations that have been successfully applied to modify both aromatic and non-aromatic azaheterocyclic substrates [30–32]. At this time, this strategy was put into practice only for the alkylation of 4*H*-imidazole 3-oxides (via the Grignard addition/oxidation reaction sequence) [33]. However, there have not been any examples of heteroarylation reported so far.

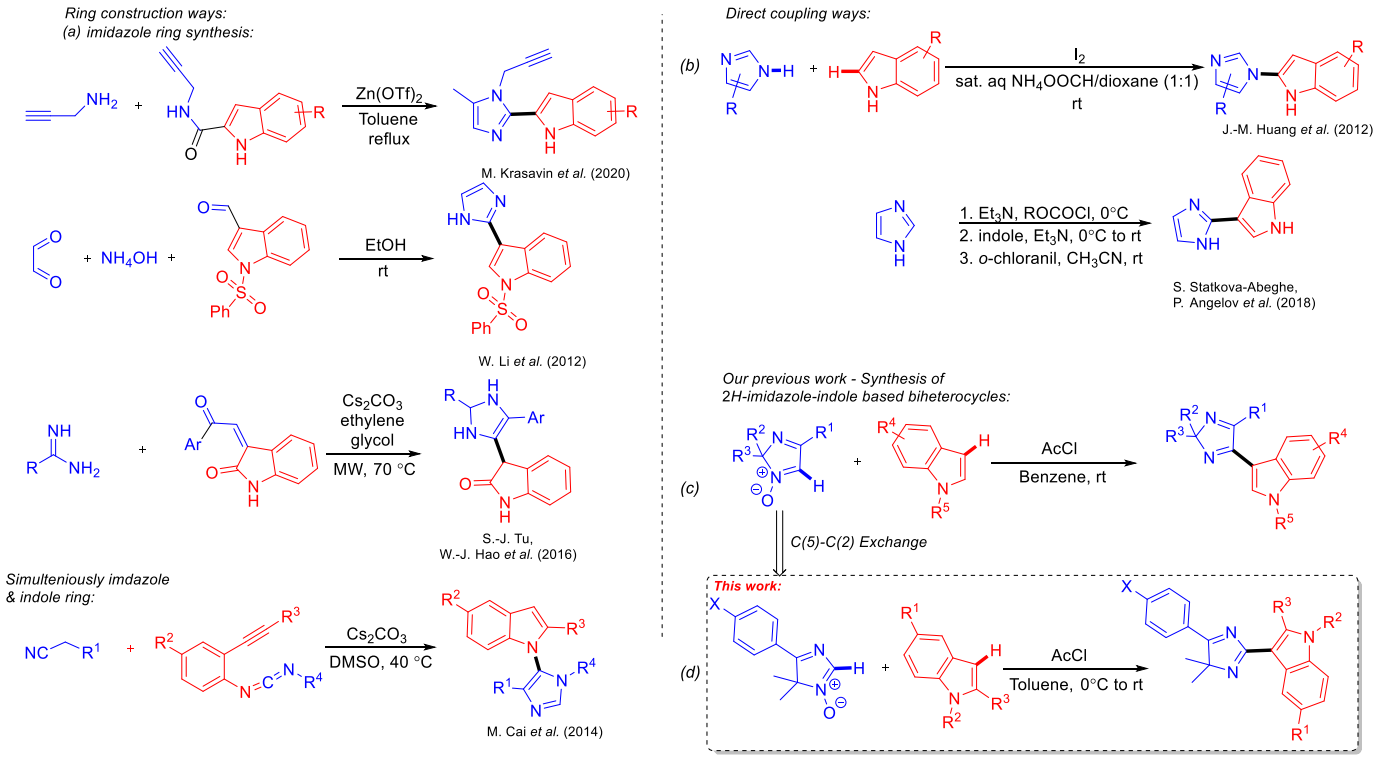

Scheme 1. Synthetic strategies towards indolyl-substituted imidazoles (Blue color indicates the imidazole ring, red color shows the indole moiety). State-of-the-art: (**a**) ring construction methods, (**b**) direct coupling methods, (**c**) our previous work, and (**d**) this work [15,16,19,21–23].

This work deals with the synthesis of indolyl-substituted imidazole derivatives utilizing S_N^H modifications of 4*H*-imidazole 3-oxides (Scheme 1d), the virtual screening of targets associated with neurodegenerative diseases, and the assessment of cytotoxic effects to evaluate the possibility of the further study and application of these compounds.

2. Materials and Methods

2.1. Experimental Procedure

Nuclear magnetic resonance (NMR) spectra were recorded on the Bruker AV-300, AV-400, DRX-500, and Bruker Avance II (400 MHz) spectrometers. All ^{1}H NMR experiments were reported in δ units, parts per million (ppm), and were measured relative to residual chloroform $DCCl_3$ (7.26 ppm) or DMSO (2.50 ppm) signals in the deuterated solvent. All ^{13}C NMR spectra were reported in parts per million (ppm) relative to $DCCl_3$ (77.16 ppm) or DMSO-d_6 (39.52 ppm) and all spectra were obtained with ^{1}H decoupling. All coupling constants *J* were reported in Hertz (Hz). The following abbreviations were used to describe peak splitting patterns (s = singlet, d = doublet, t = triplet, dd = doublet of doublet, m = multiplet, and br s = broadened singlet). The mass spectra were recorded on a mass spectrometer, SHIMADZU GCMS-QP2010 Ultra, with sample ionization by electron

impact (EI). The IR spectra were recorded using a Fourier-transform infrared spectrometer (Bruker Corporation, 40 Manning Rd, Billerica, MA, USA) equipped with a diffuse reflection attachment. The elemental analysis was carried out on a Perkin Elmer Instrument equipped with the CHN PE 2400 II analyzer and on an automatic CNS analyzer EuroEA 3000. The UV–Vis spectra were obtained for EtOH solutions using a Hewlett-Packard HP 8453 spectrophotometer. The melting points were determined on the FP 81 HT instrument "METTLER TOLEDO". The course of the reactions was monitored by TCL on 0.25 mm silica gel plates (60F 254).

Toluene, hexachloroacetone, acetone, chlorobenzene, PEG-400, 2-Me-THF, hexane, AcCl, TMS-Cl, ethyl chloroformate, oxalyl dichloride, EtOH, sodium bicarbonate, ethyl acetate, and Na_2SO_4 were purchased from Sigma-Aldrich and used as received.

Moreover, 2-(hydroxyamino)-2-methyl-1-phenylpropan-1-one (**1a**), 1-(4-bromophenyl)-2-(hydroxyamino)-2-methylpropan-1-one (**1b**), and 1-(4-fluorophenyl)-2-(hydroxyamino)-2-methylpropan-1-one (**1c**), were prepared according to a literature procedure [34,35].

2.1.1. Synthesis of 1-Hydroxy-2,5-Dihydroimidazoles **2a–c** and 4*H*-Imidazole 3-Oxides **3a–c**

First, 1-hydroxy-5,5-dimethyl-4-phenyl-2,5-dihydro-1*H*-imidazole (**2a**) was synthesized according to a slightly modified literature procedure [36]. To a suspension of 8.62 g (40 mmol) of crystallized 2-(hydroxyamino)-2-methyl-1-phenylpropan-1-one hydrochloride **1a** in 25 mL of EtOH, 30% aqueous ammonia solution (15 mL) was quickly added and the mixture was stirred until a solution formed, after which 23.5 mL of 20% aqueous formaldehyde solution was added in one portion. The mixture was shaken until a homogeneous solution was formed and placed in a cold-water bath for 1 min (to prevent boiling due to an exothermic reaction). After the beginning of the formation of a precipitate of the product, the reaction flask was kept for 15 h at room temperature and 1 d at +2 °C. The precipitate was triturated, filtered off, washed with cold 40% aqueous EtOH (2 × 5 mL), and dried in a vacuum to a constant weight. Colorless needles. Yield: 38.12 mmol (7.252 g, 95%). Lit. yield: 26.08 mmol (4.962 g, 65%), mp = 183–185 °C (lit. mp = 184–185 °C). The ^{1}H NMR spectrum of 1-hydroxy-3-imidazoline **2a** corresponds to the literature one [36].

4,4-Dimethyl-5-phenyl-4*H*-imidazole 3-oxide (**3a**). To a solution of 760 mg (4 mmol) of *N*-hydroxy derivative **2a** in 25 mL of chloroform, manganese dioxide was added (1.391 g, 16 mmol), and the reaction mixture was intensively stirred for 20 min (monitoring the conversion of the starting substrate by TLC). The reaction mixture was filtered through a glass filter with fine pores, the oxidant precipitate was washed with $CHCl_3$ (3 × 3 mL), the combined filtrate was evaporated, and the yellow oily residue was shaken with 5 mL of hexane and cooled at −12 °C for 1 d. The precipitate was triturated, quickly filtered on a cold filter, and washed with ice-cold hexane (3 mL). Dark yellow crystals. Yield: 3.40 mmol (640 mg, 85%). Lit. yield 2.80 mmol (527 mg 70%), mp = 70–72 °C (lit. mp = 71–73 °C). The ^{1}H and ^{13}C NMR spectra of the sample corresponded to the spectra given in the literature [37].

General procedure for the synthesis of 4-(4-halophenyl)-1-hydroxy-5,5-dimethyl-2,5-dihydro-1*H*-imidazoles (Supplementary Materials, **2b,c**). To a vigorously stirred suspension of 20 mmol of 2-hydroxylaminoketone hydrochloride, **1b,c** in 18 mL of EtOH ammonium acetate (6.160 g, 80 mmol) was added, and, after 3 min, 6.00 g (40 mmol) of 20% aq HCHO was added dropwise to the resulting thick suspension. It was kept for 6 h at room temperature; the solvent was evaporated to a volume of 5 mL. Water (60 mL) was added to the residue, the mixture was shaken until the oily residue solidified, the precipitate was triturated till crystals formed, and the mixture was cooled at +3 °C for 72 h. The precipitate was filtered off, washed with ice water (2 × 10 mL), and dried under a vacuum to a constant weight.

4-(4-Bromophenyl)-1-hydroxy-5,5-dimethyl-2,5-dihydro-1*H*-imidazole (**2b**). Colorless fine needle-shaped crystals. Yield 19.44 mmol (5.230 g, 97%), mp = 142–143 °C (Hexane/EtOAc, 1:1). R_f 0.5 ($CHCl_3$/MeOH, 10: 1). ^{1}H NMR (400 MHz, $DCCl_3$): δ 7.76 (br s,

1H); 7.62 (d, *J* = 7.5 Hz, 2H); 7.52 (d, *J* = 7.5 Hz, 2H); 4.98 (s, 2H); 1.43 (s, 6H) ppm. ^{13}C {^{1}H} NMR (100 MHz, $DCCl_3$): δ 174.7 (C); 131.5 (CH); 129.3 (CH); 124.8 (C); 83.6 (CH_2); 77.1 (C); 74.7 (C); 23.3 (CH_3); 20.7 (CH_3) ppm. IR (solid, KBr): ν 3641, 3165 (OH), 1620, 1589 (C=N), 1462, 1072, 1005, 835 cm^{-1}. Anal. Calcd. for $C_{11}H_{13}BrN_2O$: C, 49.09; H, 4.87; Br, 29.69; N, 10.41. Found: C, 49.17; H, 5.09; Br, 29.72; N, 10.53.

4-(4-Fluorophenyl)-1-hydroxy-5,5-dimethyl-2,5-dihydro-1*H*-imidazole (**2c**). Colorless needles. Yield: 18.20 mmol (3.79 g, 91%), mp = 109-110 °C (Hexane/EtOAc, 3:2). R_f 0.55 ($CHCl_3$/MeOH, 10: 1). ^{1}H NMR (300 MHz, $DCCl_3$): δ 7.90 (br s, 1H); 7.77 (ddd, *J* = 7.5, 5.0, 1.5 Hz, 2H); 7.07 (ddd, *J* = 8.0, 7.5, 1.5 Hz, 2H); 4.98 (s, 2H); 1.44 (s, 6H) ppm. ^{13}C {^{1}H} NMR (75 MHz, $DCCl_3$): δ 174.6 (C); 163.9 (d, *J* = 256 Hz, C); 129.8 (d, *J* = 9 Hz, CH); 128.8 (d, *J* = 3.2 Hz, C); 115.4 (d, *J* = 22.5 Hz, CH); 83.4 (CH_2); 74.6 (C); 22.9 (CH_3); 20.6 (CH_3) ppm. ^{19}F NMR (282.4 MHz, $DCCl_3$): δ 52.99 (s, 1F) ppm. IR (solid, KBr,): ν 3424 (OH), 1614, 1601 (C=N), 1512, 1456, 1321, 1221, 1159, 1009, 850 cm^{-1}. Anal. Calcd. for $C_{11}H_{13}FN_2O$: C, 63.45; H, 6.29; F, 9.12; N, 13.45. Found: C, 63.22; H, 6.24; F, 9.38; N, 13.34.

5-(4-Bromophenyl)-4,4-dimethyl-4*H*-imidazole 3-oxide (**3b**). To a vigorously stirred solution of 4.79 g (17.8 mmol) of 1-hydroxy-2,5-dihydroimidazole, **2b** in 50 mL of chloroform was added in one portion of manganese dioxide (3.097 g, 35.6 mmol) and the suspension was stirred for 60 min, after which 0.774 g (8.9 mmol) of fresh MnO_2 was introduced. After additional stirring for 40 min (complete conversion of the initial substrate was monitored by TLC), the inorganic precipitate was filtered through a glass filter with fine pores, washed with 5 × 5 mL of chloroform and 2 × 6 mL of a mixture of $CHCl_3$/EtOH, 5: 1, and the combined filtrate was evaporated to a thick oily residue. The latter was subjected to flash chromatography on silica gel, eluent $CHCl_3$/MeOH, 30:1, and a yellow-greenish fraction with R_f = 0.35 was collected; then, the solvent was evaporated to form a crystalline residue of **3b**.

Dark yellow long crystals. Yield 16.02 mmol (4.280 g, 90%), mp = 136.5 °C (dec., hexane-EtOAc, 2:1). R_f 0.8 ($CHCl_3$/MeOH, 10: 1). ^{1}H NMR (500 MHz, $DCCl_3$): δ 7.78 (s, 1H); 7.76 (d, *J* = 8.5 Hz, 2H); 7.55 (d, *J* = 8.5 Hz, 2H); 1.61 (s, 6H) ppm. ^{13}C {^{1}H} NMR (125 MHz, $DCCl_3$): δ 176.05 (C); 138.26 (CH); 132.20 (CH); 129.27 (C); 128.05 (CH); 126.36 (C); 79.13 (C); 23.68 (CH_3) ppm. IR (solid, KBr): ν 1614, 1583 (C=N), 1522 (C=N-C=N-O), 1491, 1468, 1456, 1267, 1068, 1003, 831, 754 cm^{-1}. UV (in EtOH, (lg ε)): λ 241 (3.74), 363 (4.05) nm. Anal. Calcd. for $C_{11}H_{11}BrN_2O$: C, 49.46; H, 4.15; Br, 29.91; N, 10.49. Found: C, 49.81; H, 4.02; Br, 29.72; N, 10.45.

5-(4-Fluorophenyl)-4,4-dimethyl-4*H*-imidazole 3-oxide (**3c**). One portion of 3.48 g (40 mmol) of manganese dioxide was added to a solution of 4.160 g (20 mmol) of 1-hydroxy-2,5-dihydroimidazole **2c** in 50 mL of chloroform and the suspension was intensively stirred for 45 min, after which 0.87 g (10 mmol) of fresh MnO_2 was added. Again, the addition of a portion of fresh MnO_2 (0.87 g, 10 mmol) was repeated after stirring the mixture for 1 h. The completeness of the initial substrate's conversion was monitored by TLC. The total duration of stirring of the reaction mixture was 5.5 h. The precipitate of inorganics was filtered off through a glass filter with fine pores, washed with 5 × 8 mL of $CHCl_3$ and 8 mL of $CHCl_3$/EtOH, 5:1, and the combined filtrate was evaporated until the residue began to crystallize. The semisolid substance was triturated with 15 mL of hexane and the mixture was cooled at +3 °C for 1 d. The precipitate of the product was quickly filtered off on a cold filter, washed with ice-cold hexane (2 × 10 mL), and dried in a vacuum to a constant weight.

Yellow-orange needles. Yield: 18.73 mmol (3.862 g, 94%), mp = 115–116 °C (hexane). R_f 0.7 ($CHCl_3$/MeOH, 10:1). ^{1}H NMR (300 MHz, $DCCl_3$): δ 7.98–7.87 (m, 2H); 7.78 (s, 1H); 7.15–7.07 (m, 2H); 1.61 (s, 6H) ppm. ^{13}C {^{1}H} NMR (150 MHz, $DCCl_3$): δ 176.4 (C); 164.6 (d, *J* = 253.5 Hz, C); 138.4 (CH); 129.1 (d, *J* = 9 Hz, CH); 126.9 (d, $^{4}J_{CF}$ = 3 Hz, C); 116.3 (d, *J* = 22.5 Hz, CH); 79.1 (C); 23.8 (CH_3) ppm. ^{19}F NMR (282 MHz, $DCCl_3$): δ 55.68 (s, 1F) ppm. IR (solid, KBr): ν 1603 (C=N), 1527 (C=N-C=N-O), 1512, 1227, 843, 573 cm^{-1}. UV (in EtOH,

(lg ε)): λ 233 (3.86), 276 (3.44), 359 (4.07) nm. Anal. Calcd. for $C_{11}H_{11}FN_2O$: C, 64.07; H, 5.38; F, 9.21; N, 13.58. Found: C, 64.09; H, 5.34; F, 9.53; N, 13.66.

2.1.2. General Procedure for the Synthesis of Hydrochloride Salt of Indolyl Imidazole Derivatives (**5a–d**)

To a vigorously stirred mixture of 4*H*-imidazole-3-oxide **3a** (0.5 mmol) and indole, **4a–e** (0.5 mmol) in toluene (5 mL) at 0 °C acetyl chloride (0.5 mmol) was added. Subsequently, the resulting mixture was warmed to room temperature and subjected to continued stirring for an additional 30 min. Then, the resulting precipitate **3** was filtered off and washed with hexane (10 mL).

3-(4,4-Dimethyl-5-phenyl-4*H*-imidazol-2-yl)-1-methyl-1*H*-indole hydrochloride (**5a**). Light-brown solid. Yield: 0.24 mmol (81 mg, 48%), mp = 138–139 °C. R_f 0.12 (hexane/EtOAc, 7:3). ^{1}H NMR (400 MHz, DMSO-d_6): δ 7.92–7.90 (m, 2H); 7.79 (d, *J* = 7.9 Hz, 1H); 7.53–7.50 (m, 2H); 7.41 (d, *J* = 8.2 Hz, 1H); 7.33 (s, 1H); 7.16 (t, *J* = 8.2 Hz, 1H); 7.04 (t, *J* = 8.2 Hz, 1H); 6.34 (s, 1H); 3.76 (s, 3H); 1.53 (s, 3H), 1.41 (s, 3H) ppm. ^{13}C {^{1}H} NMR (DMSO-d_6): δ 174.4; 169.6; 136.9; 132.3; 130.6; 128.6; 128.3; 127.9; 126.5; 121.2; 120.3; 118.8; 111.4; 109.6; 87.6; 74.1; 32.4; 19.1 ppm. IR (DRA): ν 3053, 2933, 1761, 1614, 1463, 1367, 1319, 1212, 1072, 1009, 940, 821, 734, 698, 598 cm^{-1}. MS (EI): m/z 301 [M] $^+$ Anal. Calcd. for $C_{20}H_{20}ClN_3$: C, 71.10; H, 5.97; Cl, 10.49; N, 12.44. Found: C, 70.96; H, 5.98; N, 12.42.

5-(Benzyloxy)-3-(4,4-dimethyl-5-phenyl-4*H*-imidazol-2-yl)-1*H*-indole hydrochloride (**5b**). Brown solid. Yield: 0.21 mmol (90 mg, 42%), mp = 136–137 °C. R_f 0.12 (hexane/EtOAc, 7:3). ^{1}H NMR (400 MHz, DMSO-d_6): δ 11.01 (br s, 1H); 7.94 (d, *J* = 8.7 Hz, 2H); 7.55–7.53 (m, 3H); 7.42–7.39 (m, 3H); 7.35–7. (m, 4H); 6.83 (dd, *J* = 8.8, 2.4 Hz, 1H); 6.36 (s, 1H); 5.06 (d, *J* = 6.7 Hz, 2H); 1.55 (s, 3H); 1.39 (s, 3H). ppm. ^{13}C {^{1}H} NMR (DMSO-d_6): δ 175.3; 169.6; 152.0; 137.8; 131.7; 131.6; 131.1; 128.8; 128.3; 128.1; 127.6; 127.5; 126.5; 125.0; 112.1; 112.0; 103.6; 87.4; 74.2; 69.7; 21.1; 19.1 ppm. IR (DRA): ν 3127, 2410, 1756, 1617, 1579, 1453, 1359, 1212, 1017, 921, 837, 811, 746, 675, 551 cm^{-1}. MS (EI): m/z 393 [M] $^+$. Anal. Calcd. for $C_{26}H_{24}ClN_3O$: C, 72.63; H, 5.63; Cl, 8.25; N, 9.77; O, 3.72. Found: C, 72.93; H, 5.61; N, 9.74.

3-(4,4-Dimethyl-5-phenyl-4*H*-imidazol-2-yl)-1*H*-indole hydrochloride (**5c**). Dark-brown solid. Yield: 0.32 mmol (105 mg, 65%), mp = 133–134 °C. R_f 0.1(hexane/EtOAc, 7:3).^{1}H NMR (DMSO-d_6): δ 11.18 (br s, 1H); 7.95–7.92 (m, 2H); 7.74 (d, *J* = 7.9 Hz, 1H); 7.55–7.50 (m, 2H); 7.39 (d, *J* = 8.1 Hz, 2H); 7.09 (t, *J* = 7.5 Hz, 1H); 6.99 (t, *J* = 7.5 Hz, 1H); 1.56 (s, 3H); 1.44 (s, 3H). ppm. ^{13}C {^{1}H} NMR (DMSO-d_6): δ 172.0; 169.6; 136.5; 131.6; 131.1; 128.8; 128.1; 126.2; 121.2; 120.0; 118.7; 111.5; 94.1; 87.0; 74.2; 21.1; 19.1 ppm. IR (DRA): ν 3137, 2916, 2429, 1778, 1630, 1463, 1382, 1335, 1302, 1247, 1171, 933, 830, 756, 679 cm^{-1}. MS (EI): m/z 287 [M]$^+$. Anal. Calcd. for $C_{19}H_{18}ClN_3$: C, 70.47; H, 5.60; Cl, 10.95; N, 12.98. Found: C, 70.24; H, 5.58; N, 12.92.

Ethyl 3-(4,4-dimethyl-5-phenyl-4*H*-imidazol-2-yl)-1*H*-indole-2-carboxylate hydrochloride (**5d**). Yellow solid. Yield: 0.105 mmol (41.6 mg, 21%), mp = 70–71 °C. R_f 0.1 (hexane/EtOAc, 7:3).^{1}H NMR (400 MHz, $DCCl_3$) δ 8.96 (br s, 1H); 7.85–7.82 (m, 2H); 7.69 (d, *J* = 7.8. Hz, 1H); 7.40–7.34 (m, 3H); 7.24 (s, 1H); 7.09 (s, 1H); 6.97 (t, *J* = 7.6 Hz, 1H); 4.33 (q, *J* = 7.2, 6.4 Hz, 2H); 1.56 (s, 3H); 1.56 (s, 3H); 1.31 (t, *J* = 7.1 Hz, 3H) ppm. ^{13}C NMR (101 MHz, $DCCl_3$): δ 207.1; 176.2; 161.6; 135.9; 132.7; 130.9; 128.8; 128.1; 127.7; 125.5; 125.2; 123.6; 120.9; 118.0; 111.9; 85.4; 61.3; 31.0; 19.0; 14.5 ppm. IR (DRA): ν 3327, 2983, 1760, 1675, 1542, 1460, 1324, 1256, 1201, 1013, 908, 803, 773, 744, 694 cm^{-1}. MS (EI): m/z 359 [M] $^+$. Anal. Calcd for $C_{22}H_{22}ClN_3O_2$: C, 66.75; H, 5.60; Cl, 8.95; N, 10.61; O, 8.08. Found: C, 66.58; H, 5.61; N, 10.59.

2.1.3. General Procedure for the Synthesis of Indolyl Imidazole Derivatives (**6e–h**)

To a vigorously stirred mixture of 4*H*-imidazole-3-oxide **3a–c** (0.5 mmol) and indole, **4a–e** (0.5 mmol) in toluene (5 mL) at 0 °C acetyl chloride (0.5 mmol) was added. Subsequently, the resulting mixture was warmed to room temperature and subjected to continued stirring for an additional 30 min. Then, the resulting precipitate **5** was filtered off, dissolved in EtOH (5 mL), and quenched with $NaHCO_3$ (5% w/v H_2O) to obtain pH 7–8. Water was

added (50 mL) and the resulting mixture was extracted with EtOAc (3 × 15 mL), dried over Na_2SO_4, and evaporated in vacuo. Then, the resulting crude solid was purified by manual column chromatography using Hexane/EtOAc (8/2) as an eluent and the formed eluate was evaporated in vacuo to obtain compounds **6** as solids.

3-(5-(4-Bromophenyl)-4,4-dimethyl-4*H*-imidazol-2-yl)-1*H*-indol-5-ol (**6e**). Dark-green solid. Yield: 0.43 mmol (162.3 mg, 85%), mp = 135–136 °C. R_f 0.28 (hexane/EtOAc, 7:3). ^{1}H NMR (400 MHz, $DCCl_3$): δ 8.08 (s, 1H); 7.89 (d, *J* = 8.6 Hz, 2H); 7.71 (dd, *J* = 5.7, 3.3 Hz, 3H); 7.53 (dd, *J* = 5.7, 3.4 Hz, 3H); 6.35 (s, 1H); 1.60 (s, 3H); 1.52 (s, 3H). ppm. ^{13}C {^{1}H} NMR (101 MHz, $DCCl_3$): δ 170.3; 150.1; 132.3; 132.0; 131.6; 130.6; 129.8; 125.5; 113.1; 112.5; 112.3; 111.9; 107.0; 105.2; 89.0; 25.0; 19.4. ppm. IR (DRA): ν 3327, 2925, 2855, 1729, 1607, 1581, 1464, 1381, 1274, 1123, 1072, 935, 795, 699, 650 cm^{-1}. MS (EI): m/z 381 [M]$^+$, 383 [M+2]$^+$. Anal. Calcd. for $C_{19}H_{16}BrN_3O$: C, 59.70; H, 4.22; Br, 20.90; N, 10.99; O, 4.19. Found: C, 59.66; H, 4.23; N, 11.01.

3-(5-(4-Fluorophenyl)-4,4-dimethyl-4*H*-imidazol-2-yl)-1*H*-indole (**6f**). Light-brown solid. Yield: 0.32 mmol (97.6 mg, 64%), mp = 185–186 °C. R_f 0.3 (hexane/EtOAc, 7:3). ^{1}H NMR (400 MHz, $DCCl_3$): δ 8.25 (s, 1H); 7.92 (dd, *J* = 8.6, 5.6 Hz, 2H); 7.86 (d, *J* = 7.9 Hz, 1H); 7.34 (d, *J* = 7.7 Hz, 2H); 7.18–7.11 (m, 3H); 6.40 (s, 1H); 1.61 (s, 3H); 1.54 (s, 3H). ppm. ^{13}C {^{1}H} NMR (101 MHz, $DCCl_3$): δ 170.2; 164.4 (d, *J* = 251.4 Hz); 136.7; 130.4 (d, *J* = 8.5 Hz); 129.0 (d, *J* = 4.0 Hz); 126.7; 124.1; 123.9; 122.6; 122.4; 120.7; 120.1; 115.8 (d, *J* = 21.7 Hz); 111.2; 88.4; 25.1; 19.3 ppm. ^{19}F NMR (376 MHz, $DCCl_3$) δ -114.11 (F) ppm. IR (DRA): ν 3327, 1748, 1604, 1509, 1458, 1430, 1367, 1204, 1150, 1008, 845, 813, 746, 639, 588 cm^{-1}. MS (EI): m/z 305 [M] $^+$. Anal. Calcd. for $C_{19}H_{16}FN_3$: C, 74.74; H, 5.28; F, 6.22; N, 13.76. Found: C, 74.49; H, 5.29; N, 13.74.

3-(5-(4-Fluorophenyl)-4,4-dimethyl-4*H*-imidazol-2-yl)-1-methyl-1*H*-indole (**6g**).

Note: in ^{13}C NMR, one signal of the aromatic carbon atom is missing, probably due to overlapping in the area of 130–120 ppm. Light-brown solid. Yield: 0.475 mmol (152 mg, 95%), mp = 156–157°C. R_f 0.32 (hexane/EtOAc, 7:3).^{1}H NMR (400 MHz, $DCCl_3$): δ 7.95 (dd, *J* = 8.6, 5.5 Hz, 2H); 7.89 (d, *J* = 7.9 Hz, 1H); 7.33 (m, 2H); 7.21–7.15 (m, 3H); 6.42 (s, 1H), 3.80 (s, 3H); 1.64 (s, 3H); 1.57 (s, 3H). ppm. ^{13}C {^{1}H} NMR (101 MHz, $DCCl_3$): δ 174.9; 170.5; 164.7 (d, *J* = 251.5 Hz); 137.8; 130.7 (d, *J* = 8.5 Hz); 129.4 (d, *J* = 3.3 Hz); 128.7; 127.4; 122.3; 121.1; 120.0; 116.1 (d, *J* = 21.7 Hz); 109.7; 88.6; 75.2; 33.3; 19.7. ppm. ^{19}F NMR (376 MHz, $DCCl_3$): δ -109.92 ppm. IR (DRA): ν 2971, 1749, 1614, 1505, 1367, 1318, 1212, 1151, 1097, 1072, 1009, 841, 740, 639, 563 cm^{-1}. MS (EI): m/z 319 [M] $^+$. Anal. Calcd. for $C_{20}H_{18}FN_3$ C, 75.21; H, 5.68; F, 5.95; N, 13.16. Found: C, 75.45; H, 5.67; N, 13.18.

5-(Benzyloxy)-3-(5-(4-fluorophenyl)-4,4-dimethyl-4*H*-imidazol-2-yl)-1*H*-indole (**6h**). Light-brown solid. Yield: 0.4 mmol (167 mg, 81%), mp = 194–195 °C. R_f 0.35 (hexane/EtOAc, 7:3).^{1}H NMR (400 MHz, $DCCl_3$): δ 8.41 (s, 1H); 7.91 (dd, *J* = 8.6, 5.4 Hz, 2H); 7.47 (dd, *J* = 7.1, 2.2 Hz, 3H); 7.38 (m, 3H); 7.14 (t, *J* = 8.6 Hz, 2H); 7.04 (t, *J* = 7.9 Hz, 1H); 6.73 (d, *J* = 7.7 Hz, 1H); 6.38 (s, 1H); 5.20 (s, 2H); 1.60 (s, 3H); 1.53 (s, 3H). ppm. ^{13}C {^{1}H} NMR (101 MHz, $DCCl_3$): δ 174.8; 170.2; 164.4 (d, *J* = 251.6 Hz); 145.4; 137.2; 130.4 (d, *J* = 8.6 Hz); 129.0 (d, *J* = 3.4 Hz); 128.9; 128.7; 128.3; 128.1; 128.0; 127.4; 123.4; 120.5; 115.8 (d, *J* = 21.7 Hz); 113.7; 103.5; 88.4; 70.4; 21.3; 19.4 ppm. ^{19}F NMR (376 MHz, $DCCl_3$) δ -114.18. ppm. IR (DRA): ν 3638, 3328, 2955, 1741, 1574, 1504, 1445, 1369, 1261, 1223, 1099, 1005, 843, 812, 787 cm^{-1}. MS (EI): m/z 411 [M] $^+$. Anal. Calcd. for $C_{26}H_{22}FN_3O$: C, 75.89; H, 5.39; F, 4.62; N, 10.21; O, 3.89. Found: C, 75.91; H, 5.38; N, 10.26.

2.2. Molecular Docking Studies

To evaluate potential in silico biological activity, protein–ligand complexes with known inhibitors were downloaded from the RCSB database: (1) BACE1 in complex with CHEMBL4473080 (IC_{50} = 1.7 nM, PDB: 6jse); (2) BChE in complex with SCHEMBL34046 (IC_{50} = 300 nM, PDB: 6eqp); (3) CK1δ in complex with CHEMBL489156 (IC_{50} = 1000 nM, PDB: 1eh4); (4) AChE in complex with CHEMBL95 (IC_{50} = 105 nM, PDB: 7e3i).

Molecular docking was carried out in the selected target proteins in the Arguslab 4.0.1 software using the Lamarckian genetic algorithm GADock and the empirical scor-

ing function AScore with default parameters. Binding sites were defined relative to the corresponding native ligands. Validation of the docking protocol was carried out by re-docking native ligands with following results: $RMSD_{6JSE}$ = 1.98 Å, $RMSD_{6EQP}$ = 1.60 Å, $RMSD_{1EH4}$ = 2.00 Å, $RMSD_{7E3I}$ = 1.98 Å. Docking scores for native ligands are also given in Table 1.

Table 1. Results from the protein–ligand docking for targets responsible for the progression of neurodegenerative diseases (Bold for the best docking score).

Structure	Docking Score (kcal/mol)			
	BACE1 6jse	**BChE 6eqp**	**CK1δ 1eh4**	**AChE 7e3i**
5a	−11.60	−10.96	−9.78	**−13.57**
5b	**−12.57** *	−11.58	**−13.09**	−13.33
5d	−10.04	**−12.89**	−11.53	−12.42
6g	−10.77	−10.66	−10.21	−11.59
6h	−11.27	−12.22	−10.99	−12.69
CHEMBL4473080	−11.27	-	-	-
SCHEMBL34046	-	−8.93	-	-
CHEMBL489156	-	-	−9.45	-
CHEMBL95	-	-	-	−8.50

* Ligands with the lowest (best) docking score for each target are marked in bold.

2.3. In Vitro Studies

2.3.1. Cell Culture

Experiments were carried out on cultured human embryonic kidney 293 cells (Hek-293, ATCC CRL 1573) [38] obtained from a shared research facility, the "Vertebrate Cell Culture Collection" (Institute of Cytology RAS, St. Petersburg, Russia). The cells were cultured using DMEM/F-12 medium containing 10% fetal bovine serum (FBS) at 37 °C, 5% CO_2 and 98% humidity. Subculturing using 0.25% trypsin solution was performed when the culture reached ≥ 90% confluency. DMEM/F-12 and FBS Qualified were purchased from Gibco™, Thermo Fisher Scientific, USA. Trypsin was purchased from Biolot Ltd., St. Petersburg, Russia.

2.3.2. Viability Assessment

The compounds were dissolved in DMSO. The solutions were diluted with DMEM/F-12 culture medium with 10% fetal bovine serum to the studied concentrations: 4, 8, 16, 32, 64, 128, 256, 512 μM (**5a**, **5d**) and 2–256 μM (**5b**, **6g** and **6h**). In all cases, the concentration of DMSO in the final solution did not exceed 1%.

Cells were seeded in 96-well plates at a concentration of 4×10^3 cells per well. After 24 h, test compounds were added to the wells in a given concentration range. Then, the cells were incubated for 24 h, after which a solution of MTT (3-(4,5-dimethyl-2-thiazolyl)-2,5-diphenyl-2*H*-tetrazolium bromide) was added to the cultures at 20 μL (5 mg/mL) per well. After 2 h, the medium was removed from the wells and 200 μL of a mixture of DMSO and propanol-2, 1:1, was added. Optical density was measured on a plate spectrophotometer at a wavelength of 570 nm.

2.3.3. Statistical Analysis

Statistical data processing was carried out in the RStudio program (2022.07.1+554) using the R package (version 4.2.1). The cytotoxicity index (IC_{50}) was calculated by plotting dose–response curves using the "drc" package [39].

3. Results and Discussion

3.1. Synthesis

The synthetic study was started by expanding the range of heterocyclic substrates **3**, 4*H*-imidazole 3-oxide derivatives, to be involved in the key heteroarylation reaction. It should be noted that cyclic aldonitrones in the series of 4*H*-imidazoles are extremely rare, with only three examples of such compounds being reported in the literature [37,40]. By modifying the procedure for the preparation of 5-aryl-substituted 4*H*-imidazole 3-oxides based on available 2-hydroxylamino ketones **1**, azaheterocyclic substrates **3** were obtained in almost quantitative yields via two-stage synthesis (Scheme 2).

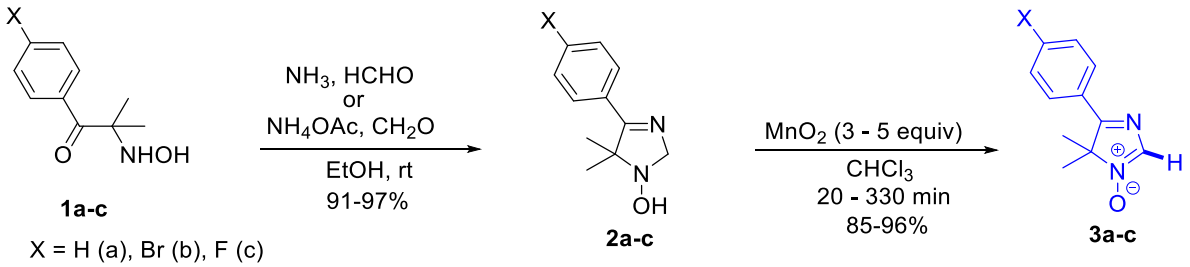

Scheme 2. General route to 5-aryl-4,4-dimethyl-4*H*-imidazole 3-oxides **3** (Blue color indicated the 4*H*-imidazole 3-oxides, which is involved in the C-H/C-H couplings).

Next, novel indolyl-derived imidazoles **6** were prepared by using the direct transition metal-free C-H/C-H coupling reactions of 4*H*-imidazole 3-oxides **3** with indoles **4**. These transformations were shown to proceed according to the "addition–elimination" scheme of the nucleophilic substitution of hydrogen (S_N^H AE). According to the previously reported synthetic scheme for the C-H/C-H coupling reactions of 2*H*-imidazole 1-oxide with indoles [26], which proceeded via the same S_N^H AE scheme, the C(3) atom of indole is involved in the formation of new C-C bonds. However, there are a few examples in which the C(2) atom of the indole ring is a nucleophilic center, with special conditions being required to provide the C-C bond formation therein [41]. As a result, the desired indolyl imidazoles were isolated as hydrochloride salts **5**. The latter were shown to be readily removed by quenching them with $NaHCO_3$ (5% w/v in H_2O) to give the corresponding base forms **6** (Scheme 3).

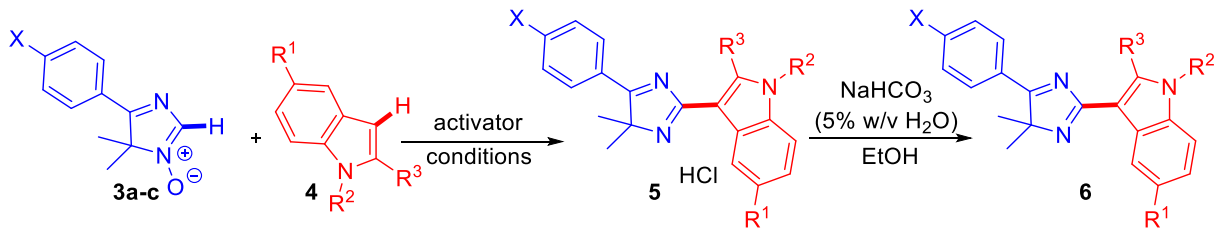

X = H (a), Br (b), F (c)

5a: X = H, R^1 = H, R^2 = Me, R^3 = H, 48%
5b: X = H, R^1 = OBn, R^2 = H, R^3 = H, 42%
5c: X = H, R^1 = H, R^2 = H, R^3 = H, 65%
5d: X = H, R^1 = H, R^2 = H, R^3 = COOEt, 21%

6e: X = Br, R^1 = OH, R^2 = H, R^3 = H, 85%
6f: X = F, R^1 = H, R^2 = H, R^3 = H, 64%
6g: X = F, R^1 = H, R^2 = Me, R^3 = H, 95%
6h: X = F, R^1 = OBn, R^2 = H, R^3 = H, 81%

Scheme 3. Transition metal-free C-H/C-H coupling of 4*H*-imidazole 3-oxides **3** (blue) with indoles **4** (red).

To define the optimal conditions, the reaction between 4*H*-imidazole 3-oxide **3a** and 1-methylindole **4a** was chosen as a model one (Scheme 4). The key reaction parameters, such as time, activating agent, temperature and solvents, were evaluated (for detailed optimization, see Supplementary Materials). Firstly, the desired compound **5a** was obtained in a 25% yield in toluene, using acetyl chloride as an activating agent (Table 2, Entry 1). Reducing the reaction time from 4 to 0.5 h led to a significant increase in the yield to

48% (Table 2, Entries 2 and 3). Most likely, the salt was not sufficiently stable in the reaction conditions. On the other hand, the use of other activating agents, such as ethyl chloroformate or oxalyl chloride, led either to the trace yield of **5a** or to only the starting materials (Table 2, Entries 4 and 5). All attempts to replace toluene with a greener solvent, such as PEG-400 or 2-MeTHF (Table 2, Entries 6 and 9), provided a lower yield of the reaction products.

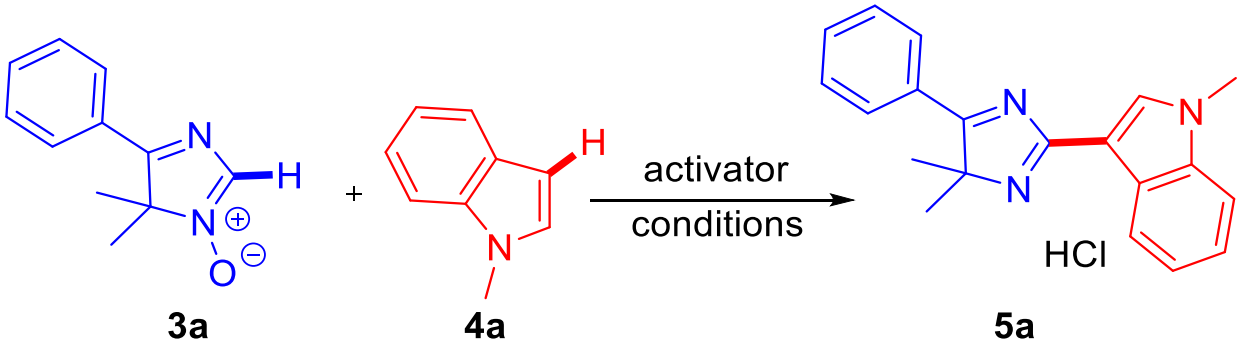

Scheme 4. Model reaction for optimization of C-H/C-H coupling of 4*H*-imidazole 3-oxide **3a** (blue) with indole **4a** (red).

Table 2. Optimization of the C-H/C-H coupling reaction of 4*H*-imidazole 3-oxide **3a** with indole **4a** (bold for the best result of optimization).

Entry [a]	Solvent	Activating Agent (Equiv)	Temperature (°C)	Time (h)	Yield (%)
1	Toluene	AcCl (1.0)	0 °C to rt	4	25 [b]
2	**Toluene**	**AcCl (1.0)**	**0 °C to rt**	**0.5**	**48 [b]**
3	Toluene	AcCl (1.0)	0 °C to rt	2	35 [b]
4	Toluene	Ethyl chloroformate (1.0)	0 °C to rt	0.5	20 [b]
5	Toluene	Oxalyl chloride (1.0)	0 °C to rt	0.5	0 [c]
6	PEG-400	AcCl (1.0)	0 °C to rt	4	10 [b]
7	Hexane/Toluene (1/1)	AcCl (1.0)	0 °C to rt	4	15 [b]
8	2-Me-THF	AcCl (1.0)	0 °C to rt	4	0 [c]
9	Anisole	AcCl (1.0)	0 °C to rt	4	0 [c]

[a] All reactions were carried out using 1 mmol of each substrate. [b] Isolated yield. [c] The only starting materials were recovered.

With the best identified, optimal conditions in hand, eight novel indolyl-derived 4*H*-imidazoles were obtained in 21–95% yields (Figure 2). It should be noted that compounds **5a–d**, containing a phenyl ring in the imidazole moiety, are able to be isolated only as hydrochlorides, since the corresponding free forms are unstable in solutions. On the contrary, molecules **6e–h**, bearing bromine or fluorine atoms in the *para*-position of the phenyl ring, are not decomposed, but contain some impurities, and therefore need to be purified by column chromatography. All the novel compounds were fully characterized by ^{1}H, ^{13}C, ^{19}F NMR, mass spectrometry, IR and elemental analysis, with the structures being completely confirmed.

Based on the results of our previous works [26,42,43], a plausible reaction mechanism was proposed (Scheme 5, an example for coupling of **3a** and **4a**). At the first stage, acetyl chloride is attached to the *N*-oxide group of 4*H*-imidazole 3-oxide **3a** to form structure **3.1**. It is most likely to undergo the nucleophilic attack from the C-H bond of indole **4a** with the formation of intermediate **3.2**. Subsequently, the elimination of acetic acid leads to the indolyl-substituted 4*H*-imidazoles **5a** in the hydrochloride salt form.

3.2. In Silico Studies

As mentioned in the Introduction, biological targets, such as BACE1, AChE, BChE and CK1δ, are actively discussed in publications focused on the design of drug candidates for the treatment of neurodegenerative diseases. Potential biological activity regarding these target proteins was determined by molecular docking in the ArgusLab 4.0.1 [44] software based on the corresponding protein–ligand complexes BACE1, BChE, CK1δ and AChE with the known inhibitors (Figure 3).

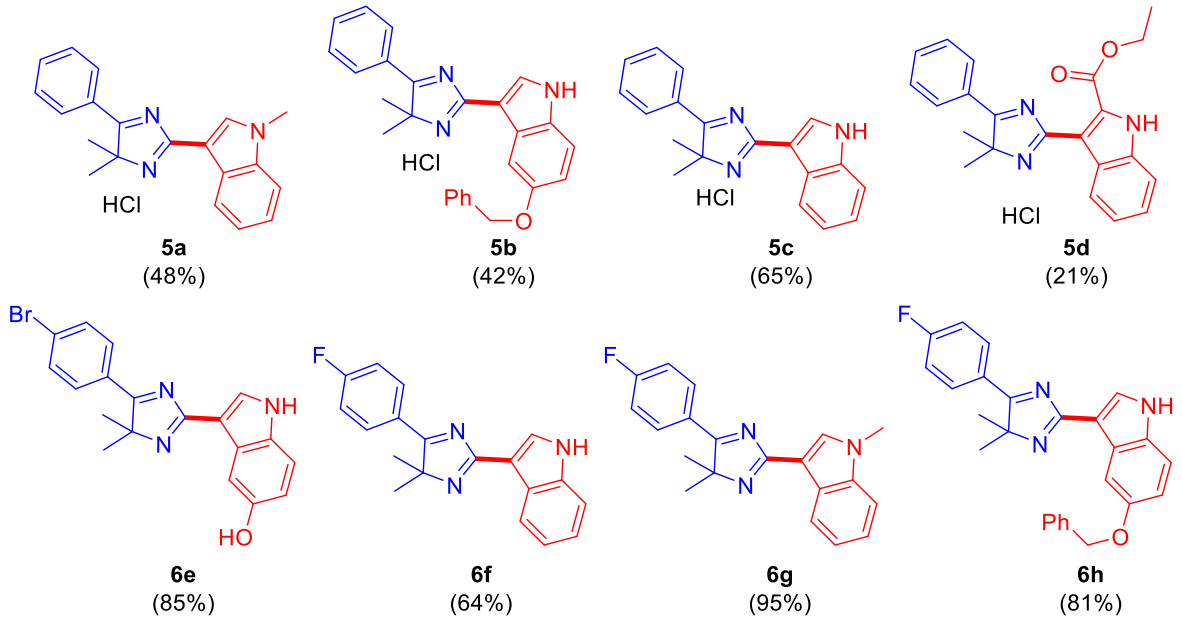

Figure 2. Structures and yields for the obtained indolyl-derived 4*H*-imidazoles. (Blue color indicates the imidazole ring, red color shows the indole moiety).

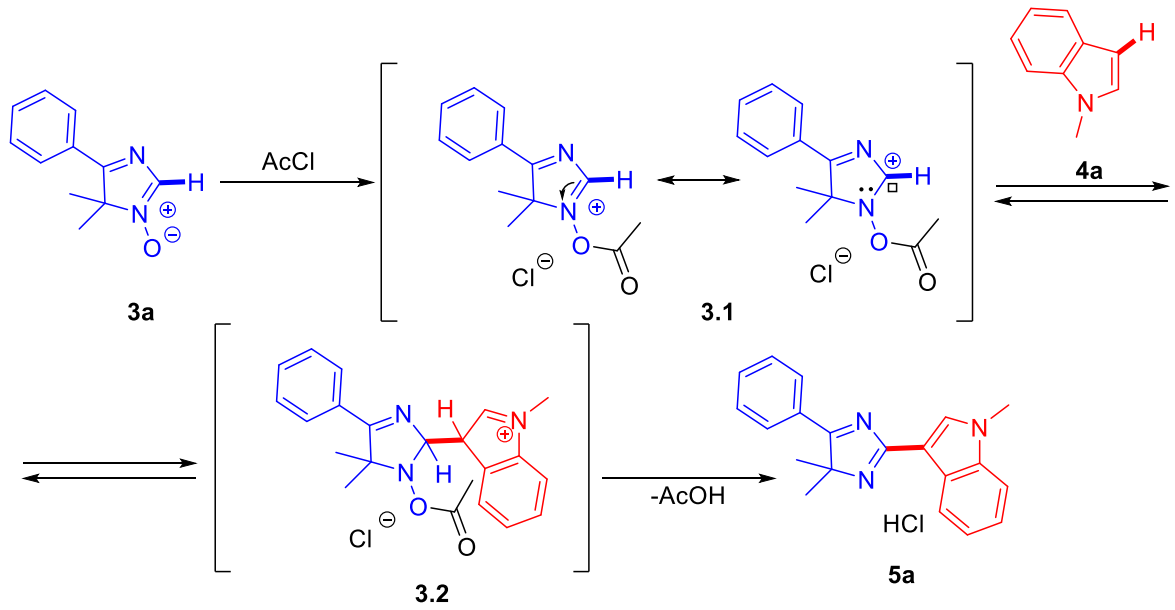

Scheme 5. Plausible mechanism for C-H/C-H coupling of 4*H*-imidazole 3-oxide **3a** (blue) with indole **4a** (red).

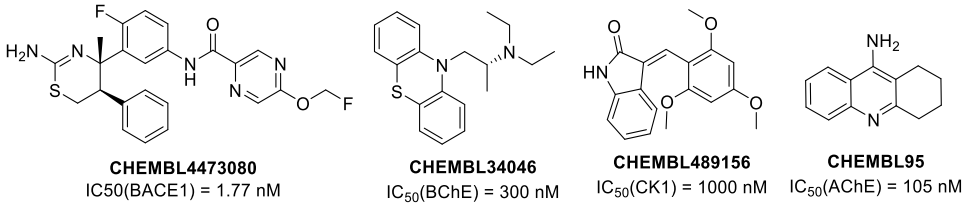

Figure 3. Examples of inhibitors of BACE1 (CHEMBL4473080, PDB: 6jse), BChE (CHEMBL34046, PDB: 6eqp), CK1δ (CHEMBL489156, PDB: 1eh4), AChE (CHEMBL95, PDB: 7e3i).

The docking results in comparison with the known inhibitors (native ligands) are presented in Table 1.

Docking scores for most compounds were found to be lower than scores for native ligands. According to SwissADME [45], all compounds have sufficient absorption, distribution, metabolism and excretion (ADME) characteristics, except for **6h**, with WlogP > 5 and satisfactory blood–brain barrier (BBB) permeability values [46] (for detailed values, see ESI). However, the calculated positions of the compounds differ from the native ligands in terms of their locations in the active sites (Figure 4a,b).

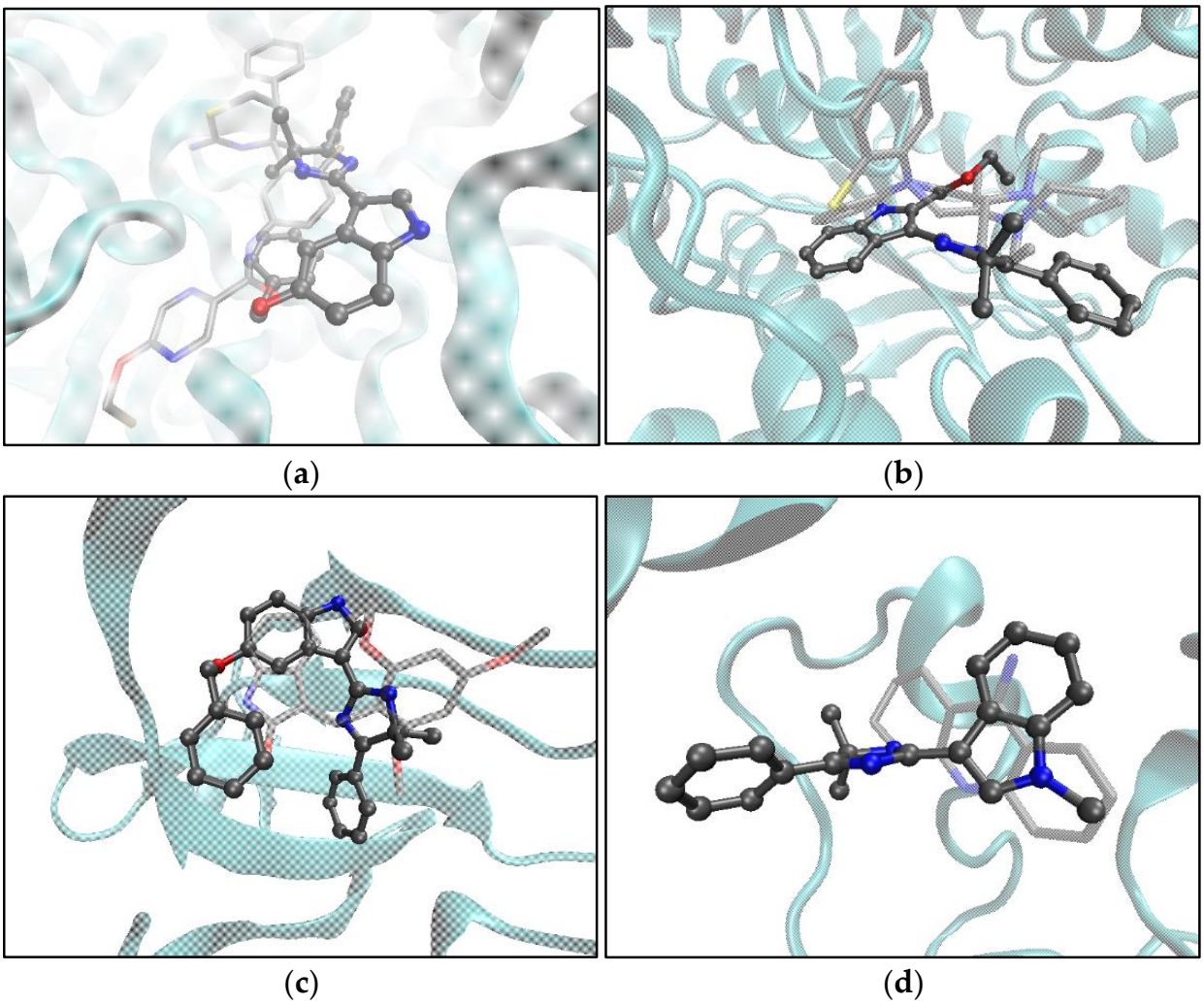

Figure 4. Leading compounds (opaque with bonds as cylinders and atoms as spheres) compared with native ligands (transparent with bonds as cylinders) in the corresponding targets (transparent, cyan): (**a**) **5b** in BACE1; (**b**) **5d** in BChE; (**c**) **5b** in CK1δ; (**d**) **5a** in AChE. – Atom colors are presented according to CPK (Corey–Pauling–Koltun) color scheme.

Docked leading compounds **5b** (Figure 5a) and **5a** (Figure 5c) in the active sites of CK1δ and AChE, respectively, were shown to have several common non-covalent interactions with respect to the corresponding native ligands (Figure 5b,d)

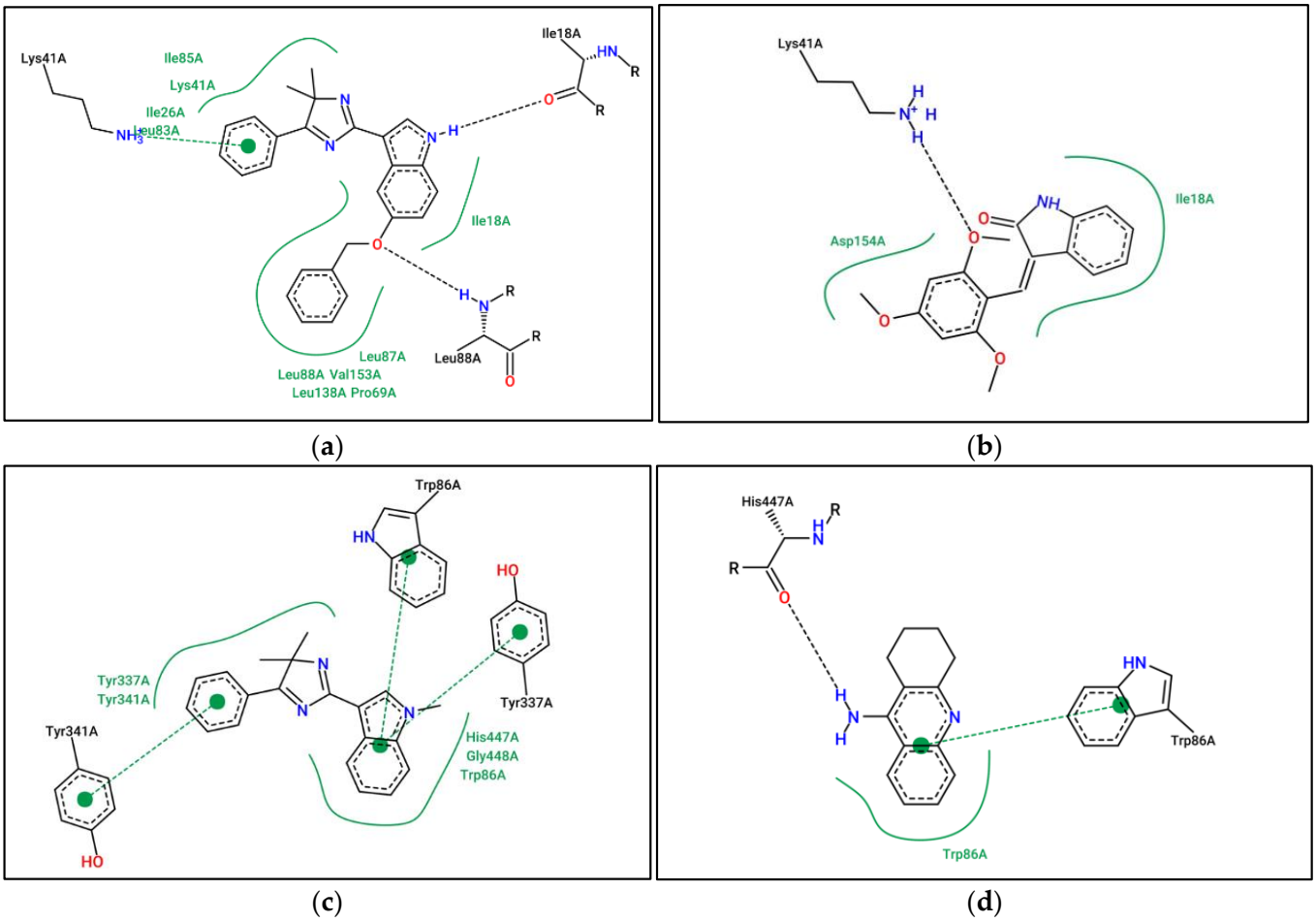

Figure 5. Two-dimensional maps of non-covalent interactions of ligands: (**a**) **5b** in CK1δ; (**b**) native inhibitor of CK1δ; (**c**) **5a** in AChE; (**d**) native ligand inhibitor of AChE.

Thus, compounds **5b** and **5a** could be regarded as the most promising inhibitors for CK1δ and AChE target proteins, respectively, which also have satisfactory calculated ADME values including BBB permeability in the series of obtained compounds.

3.3. In Vitro Studies

To evaluate the toxicity effect for the obtained compounds, the MTT test was performed on HEK-293 cells. Based on the results, the IC_{50} values were calculated (Table 3).

Table 3. Cytotoxicity index ($IC_{50} \pm SE$, n = 30) for the obtained compounds on human embryo kidney cells (HEK-293) (μM).

Entry	Compound	$IC_{50} \pm SE$
1	**5a**	306.85 ± 37.65
2	**5b**	59.58 ± 3.63
3	**5d**	66.60 ± 4.98
4	**6g**	181.68 ± 20.69
5	**6h**	>256

According to the experimental results, compounds **5b** and **5d** were found to be characterized as the most toxic for HEK-293 cells. This fact seems to limit the possibility for further applications, despite the revealed high affinity for biological targets. However, compounds **5a**, **6g** and **6h** demonstrated relatively low toxicity towards cultured cells. At the same time, the cytotoxicity index for **6h** exceeded the range of the studied concentrations, limited by the solubility of the compound. Nevertheless, at the maximum concentration of 256 μM, cell viability was already reduced by more than 30% compared to the control values. In addition, increasing cell viability at low concentrations was observed in the presence of compounds **5b** and **6h** (Figure 6).

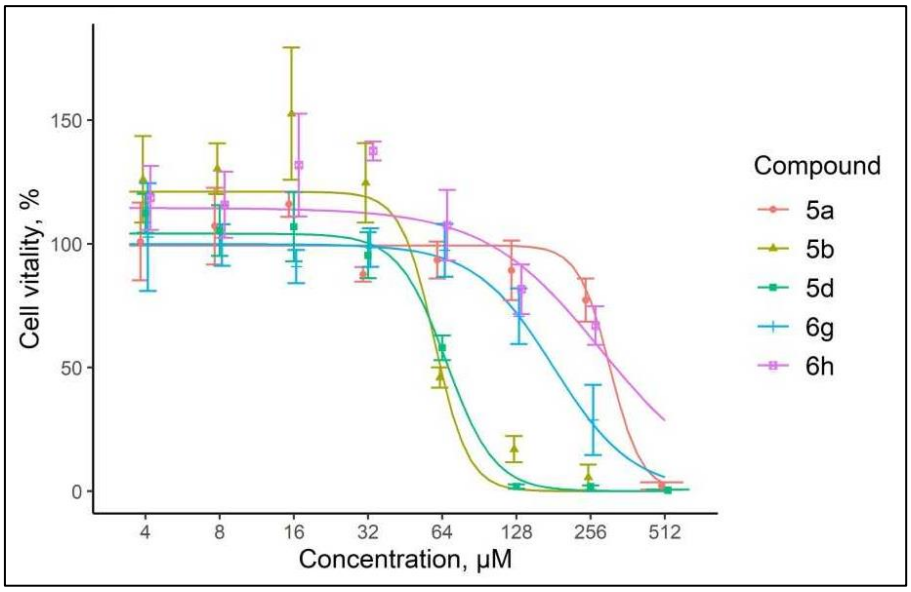

Figure 6. Dose–response curves of test compounds on human embryonic kidney cells HEK-293 (mean ± SD, n = 3).

Thus, regarding the results of both in silico and in vitro assays, compound **5a**, 3-(4,4-dimethyl-5-phenyl-4*H*-imidazol-2-yl)-1-methyl-1*H*-indole hydrochloride, could be considered as a candidate for further studies of its possible neuroprotective activity.

4. Conclusions

In summary, the S_N^H strategy has been successfully applied for the heteroarylation of 4*H*-imidazole 3-oxides for the first time to afford a series of novel indolyl-derived 4*H*-imidazoles of various architectures. Notably, 4*H*-imidazole 3-oxides have been found to be less reactive than 2*H*-imidazole 1-oxides in the same chemical transformation with indoles, possibly because of the less electrophilic character of the C(2) carbon atom in the heterocyclic system. The obtained compounds have shown satisfactory results in in silico experiments for binding to biological targets (BACE1, BChE, CK1δ, AChE) applied in the computer-aided design of drug candidates for the therapy of neurodegenerative diseases. In vitro experiments have been also performed to assess the cytotoxicity of the synthesized indolyl-derived 4*H*-imidazole 3-oxides towards healthy human cells. The leading compound bearing 5-phenyl-4*H*-imidazole and 1-methyl-1*H*-indole moieties has been defined as the candidate molecule possessing the lowest cytotoxicity (IC_{50} > 300 μM towards human embryo kidney cells, HEK-293) and highest binding energy for the protein–ligand complex (AChE, −13.57 kcal/mol). Thereby, the obtained results from sequential interdisciplinary research, including chemical design, synthesis, characterization and in silico and in vitro cytotoxicity studies, could be regarded as the basis for the further investigation of the designed compounds in enzyme and model animals, as relevant steps in the development of drug candidates.

Supplementary Materials: The following supporting information can be downloaded at: https://www.mdpi.com/article/10.3390/pr11030846/s1, Figures S1–S29: Copies of NMR spectra for **2b,c**, **3b,c**, **5a–d**, **6e–h**; Figures S30,S31: Copies of UV-VIS spectra for **3b,c**; Figures S32–S43: Copies of IR-spectra for **2b,c**, **3b,c**, **5a–d**, **6e–h**; Table S1: Optimization of reaction conditions; Table S2: Docking results.

Author Contributions: Conceptualization, O.N.C., V.N.C. and M.V.V.; methodology, E.A.N. and T.D.M.; software, I.I.B.; validation, D.G.M., A.Y.T., I.I.B. and V.V.M.; investigation, E.A.N., N.F.V., V.V.M., M.D.T., D.G.M. and A.Y.T.; data curation, T.D.M.; writing—original draft preparation, E.A.N. and T.D.M.; writing—review and editing, M.V.V. and V.N.C.; visualization, N.F.V.; supervision, M.V.V.; project administration, V.N.C. and O.N.C. All authors have read and agreed to the published version of the manuscript.

Funding: The chemical design, synthesis and characterization of indolyl-derived 4*H*-imidazoles and in vitro studies were supported by the Russian Science Foundation (Project # 20-73-10077). The in silico studies were supported by the Ministry of Science and Higher Education of the Russian Federation (Ref. # 075-15-2022-1118, dated 29 June 2022). The synthesis of starting 4*H*-imidazole *N*-oxide substrates was supported by the Ministry of Science and Higher Education of the Russian Federation (Project # 14.W03.31.0034).

Data Availability Statement: The data presented in this study are available on request from the corresponding author and co-authors.

Conflicts of Interest: The authors declare no conflict of interest.

References

1. Erkkinen, M.G.; Kim, M.-O.; Geschwind, M.D. Clinical Neurology and Epidemiology of the Major Neurodegenerative Diseases. *Cold Spring Harb. Perspect. Biol.* **2018**, *10*, a033118. [CrossRef] [PubMed]
2. Elbaz, A.; Carcaillon, L.; Kab, S.; Moisan, F. Epidemiology of Parkinson's Disease. *Rev. Neurol.* **2016**, *172*, 14–26. [CrossRef]
3. Min, Y.G.; Choi, S.-J.; Hong, Y.-H.; Kim, S.-M.; Shin, J.-Y.; Sung, J.-J. Dissociated Leg Muscle Atrophy in Amyotrophic Lateral Sclerosis/Motor Neuron Disease: The 'Split-Leg' Sign. *Sci. Rep.* **2020**, *10*, 15661. [CrossRef] [PubMed]
4. Dayalu, P.; Albin, R.L. Huntington Disease. *Neurol. Clin.* **2015**, *33*, 101–114. [CrossRef]
5. Murphy, M.P.; Hartley, R.C. Mitochondria as a Therapeutic Target for Common Pathologies. *Nat. Rev. Drug Discov.* **2018**, *17*, 865–886. [CrossRef] [PubMed]
6. Ramrao, S.P.; Verma, A.; Waiker, D.K.; Tripathi, P.N.; Shrivastava, S.K. Design, Synthesis, and Evaluation of Some Novel Biphenyl Imidazole Derivatives for the Treatment of Alzheimer's Disease. *J. Mol. Struct.* **2021**, *1246*, 131152. [CrossRef]
7. Bolcato, G.; Cescon, E.; Pavan, M.; Bissaro, M.; Bassani, D.; Federico, S.; Spalluto, G.; Sturlese, M.; Moro, S. A Computational Workflow for the Identification of Novel Fragments Acting as Inhibitors of the Activity of Protein Kinase CK1δ. *Int. J. Mol. Sci.* **2021**, *22*, 9741. [CrossRef]
8. Kaur, G.; Goyal, B. Deciphering the Molecular Mechanism of Inhibition of B-Secretase (BACE1) Activity by a 2-Amino-imidazol-4-one Derivative. *ChemistrySelect* **2022**, *7*, e202202561. [CrossRef]
9. Gujjarappa, R.; Kabi, A.K.; Sravani, S.; Garg, A.; Vodnala, N.; Tyagi, U.; Kaldhi, D.; Velayutham, R.; Singh, V.; Gupta, S.; et al. Overview on Biological Activities of Imidazole Derivatives. In *Nanostructured Biomaterials. Materials Horizons: From Nature to Nanomaterials*; Swain, B., Ed.; Springer: Singapore, 2022; pp. 135–227. ISBN 978-981-16-8399-2.
10. Wu, J.; Liu, Q.; Hu, Y.; Wang, W.; Gao, X. Discovery of Novel Procaine-Imidazole Derivative as Inhibitor of Monoamine Oxidase-B for Potential Benefit in Parkinson's Disease. *ChemistrySelect* **2020**, *5*, 10928–10932. [CrossRef]
11. Cornec, A.-S.; Monti, L.; Kovalevich, J.; Makani, V.; James, M.J.; Vijayendran, K.G.; Oukoloff, K.; Yao, Y.; Lee, V.M.-Y.; Trojanowski, J.Q.; et al. Multitargeted Imidazoles: Potential Therapeutic Leads for Alzheimer's and Other Neurodegenerative Diseases. *J. Med. Chem.* **2017**, *60*, 5120–5145. [CrossRef]
12. Nirwan, N.; Pareek, C.; Swami, V.K. Indolylimidazoles: Synthetic Approaches and Biological Activities. *Curr. Chem. Lett.* **2020**, *9*, 31–50. [CrossRef]
13. Kawano, T.; Inokuchi, J.; Eto, M.; Murata, M.; Kang, J.-H. Activators and Inhibitors of Protein Kinase C (PKC): Their Applications in Clinical Trials. *Pharmaceutics* **2021**, *13*, 1748. [CrossRef]
14. Hogendorf, A.S.; Hogendorf, A.; Popiołek-Barczyk, K.; Ciechanowska, A.; Mika, J.; Satała, G.; Walczak, M.; Latacz, G.; Handzlik, J.; Kieć-Kononowicz, K.; et al. Fluorinated indole-imidazole conjugates: Selective orally bioavailable 5-HT_7 receptor low-basicity agonists, potential neuropathic painkillers. *Eur. J. Med. Chem.* **2019**, *170*, 261–275. [CrossRef] [PubMed]
15. Bakholdina, A.; Lukin, A.; Bakulina, O.; Guranova, N.; Krasavin, M. Dual Use of Propargylamine Building Blocks in the Construction of Polyheterocyclic Scaffolds. *Tetrahedron Lett.* **2020**, *61*, 151970. [CrossRef]
16. Chen, J.; Ahn, S.; Wang, J.; Lu, Y.; Dalton, J.T.; Miller, D.D.; Li, W. Discovery of Novel 2-Aryl-4-Benzoyl-Imidazole (ABI-III) Analogues Targeting Tubulin Polymerization As Antiproliferative Agents. *J. Med. Chem.* **2012**, *55*, 7285–7289. [CrossRef] [PubMed]

17. Suvorov, N.N.; Smushkevich, Y.I.; Mar'yanovskaya, N.N.; Sulima, A.V. Indole Derivatives. LXI. Synthesis of 4(5)-(Indolyl-3)-Imidazole. *Pharm. Chem. J.* **1970**, *4*, 68–70. [CrossRef]
18. El-Nakkady, S.S.; Hanna, M.M.; Roaiah, H.M.; Ghannam, I.A.Y. Synthesis, Molecular Docking Study and Antitumor Activity of Novel 2-Phenylindole Derivatives. *Eur. J. Med. Chem.* **2012**, *47*, 387–398. [CrossRef] [PubMed]
19. Chen, K.; Dai, M.-L.; Pan, Y.-Q.; Zhang, C.; Tu, S.-J.; Hao, W.-J. Regioselective Synthesis of 3-(Imidazol-4-Yl) Indolin-2-Ones under Microwave Heating. *J. Heterocycl. Chem.* **2016**, *54*, 1479–1485. [CrossRef]
20. Hary, U.; Roettig, U.; Paal, M. Efficient Synthesis of 3-(4,5-Dihydro-1*H*-Imidazole-2-Yl)-1H-Indoles. *Tetrahedron Lett.* **2001**, *42*, 5187–5189. [CrossRef]
21. Hao, W.; Jiang, Y.; Cai, M. Synthesis of Indolyl Imidazole Derivatives via Base-Promoted Tandem Reaction of N-[2-(1-Alkynyl)Phenyl]Carbodiimides with Isocyanides. *J. Org. Chem.* **2014**, *79*, 3634–3640. [CrossRef] [PubMed]
22. Wu, W.-B.; Huang, J.-M. Highly Regioselective C–N Bond Formation through C–H Azolation of Indoles Promoted by Iodine in Aqueous Media. *Org. Lett.* **2012**, *14*, 5832–5835. [CrossRef] [PubMed]
23. Stremski, Y.; Statkova-Abeghe, S.; Angelov, P.; Ivanov, I. Synthesis of Camalexin and Related Analogues. *J. Heterocycl. Chem.* **2018**, *55*, 1589–1595. [CrossRef]
24. Liu, X.; He, K.; Gao, N.; Jiang, P.; Lin, J.; Jin, Y. A Radical-Mediated Multicomponent Cascade Reaction for the Synthesis of Azide-Biindole Derivatives. *Chem. Commun.* **2021**, *57*, 9696–9699. [CrossRef] [PubMed]
25. Bergman, J.; Renström, L.; Sjöberg, B. Synthesis of Aromatic Aldehydes via 2-Aryl-n,n'-Diacyl-4-Imidazolines. *Tetrahedron* **1980**, *36*, 2505–2511. [CrossRef]
26. Varaksin, M.V.; Utepova, I.A.; Chupakhin, O.N.; Charushin, V.N. Palladium(II)-Catalyzed Oxidative C–H/C–H Coupling and Eliminative S_N^H Reactions in Direct Functionalization of Imidazole Oxides with Indoles. *J. Org. Chem.* **2012**, *77*, 9087–9093. [CrossRef] [PubMed]
27. Vaccaro, L. Green Shades in Organic Synthesis. *Eur. J. Org. Chem.* **2020**, *2020*, 4273–4283. [CrossRef]
28. de Marco, B.A.; Rechelo, B.S.; Tótoli, E.G.; Kogawa, A.C.; Salgado, H.R.N. Evolution of Green Chemistry and Its Multidimensional Impacts: A Review. *Saudi Pharm. J.* **2019**, *27*, 1–8. [CrossRef]
29. Gujral, S.S.; Sheela, M.A.; Khatri, S.; Singla, R.K. A Focus & Review on the Advancement of Green Chemistry. *Indo Glob. J. Pharm. Sci.* **2012**, *2*, 397–408. [CrossRef]
30. Charushin, V.N.; Chupakhin, O.N. Nucleophilic C—H Functionalization of Arenes: A Contribution to Green Chemistry. *Russ. Chem. Bull.* **2019**, *68*, 453–471. [CrossRef]
31. Chupakhin, O.N.; Charushin, V.N. Recent Advances in the Field of Nucleophilic Aromatic Substitution of Hydrogen. *Tetrahedron Lett.* **2016**, *57*, 2665–2672. [CrossRef]
32. Akulov, A.A.; Varaksin, M.V.; Charushin, V.N.; Chupakhin, O.N. C(sp^2)–H Functionalization of Aldimines and Related Compounds: Advances and Prospects. *Russ. Chem. Rev.* **2021**, *90*, 374–394. [CrossRef]
33. Edeleva, M.V.; Parkhomenko, D.A.; Morozov, D.A.; Dobrynin, S.A.; Trofimov, D.G.; Kanagatov, B.; Kirilyuk, I.A.; Bagryanskaya, E.G. Controlled/Living Polymerization of Methyl Methacrylate Using New Sterically Hindered Imidazoline Nitroxides Prepared via Intramolecular 1,3-Dipolar Cycloaddition Reaction. *J. Polym. Sci. Part A Polym. Chem.* **2014**, *52*, 929–943. [CrossRef]
34. Volodarskii, L.B.; Sevast'yanova, T.K. Synthesis and properties of α-hydroxylamino ketones. *Zh. Org. Khim.* **1971**, *7*, 1687–1692.
35. Amitina, S.A.; Zaytseva, E.V.; Dmitrieva, N.A.; Lomanovich, A.V.; Kandalintseva, N.V.; Ten, Y.A.; Artamonov, I.A.; Markov, A.F.; Mazhukin, D.G. 5-Aryl-2-(3,5-Dialkyl-4-Hydroxyphenyl)-4,4-Dimethyl-4*H*-Imidazole 3-Oxides and Their Redox Species: How Antioxidant Activity of 1-Hydroxy-2,5-Dihydro-1*H*-Imidazoles Correlates with the Stability of Hybrid Phenoxyl–Nitroxides. *Molecules* **2020**, *25*, 3118. [CrossRef]
36. Kirilyuk, I.A.; Grigor'ev, I.A.; Volodarskii, L.B. Synthesis of 3-imidazolines and 3-imidazoline 3-oxides containing a hydrogen atom at C-2. *Izv. SO AN SSSR Ser. Khim.* **1989**, *2*, 99–106.
37. Grigor'ev, I.A.; Kirilyuk, I.A.; Volodarskii, L.B. NMR Spectra of Cyclic Nitrones. 4. Synthesis and ^{13}C NMR Spectra of 4*H*-Imidazole *N*-Oxides and *N*,*N*-Dioxides. *Chem. Heterocycl. Compd.* **1988**, *24*, 1355–1362. [CrossRef]
38. Russell, W.C.; Graham, F.L.; Smiley, J.; Nairn, R. Characteristics of a Human Cell Line Transformed by DNA from Human Adenovirus Type 5. *J. Gen. Virol.* **1977**, *36*, 59–72. [CrossRef]
39. Ritz, C.; Baty, F.; Streibig, J.C.; Gerhard, D. Dose-Response Analysis Using R. *PLoS ONE* **2015**, *10*, e0146021. [CrossRef]
40. Voinov, M.A.; Volodarsky, L.B. Synthesis and Properties Of *N*-[1-Hydroxyimino-2-Methyl-1-(2-Pyridyl)Prop-2-Yl]Hydroxylamine and Heterocyclic Derivatives Based on It. *Russ. Chem. Bull.* **1997**, *46*, 126–132. [CrossRef]
41. Tayu, M.; Nomura, K.; Kawachi, K.; Higuchi, K.; Saito, N.; Kawasaki, T. Direct C2-Functionalization of Indoles Triggered by the Generation of Iminium Species from Indole and Sulfonium Salt. *Chem.—A Eur. J.* **2017**, *23*, 10925–10930. [CrossRef]
42. Moseev, T.D.; Nikiforov, E.A.; Varaksin, M.V.; Charushin, V.N.; Chupakhin, O.N. Metal-Free C–H/C–H Coupling of 2 H-Imidazole 1-Oxides with Polyphenols toward Imidazole-Linked Polyphenolic Compounds. *J. Org. Chem.* **2021**, *86*, 13702–13710. [CrossRef] [PubMed]
43. Varaksin, M.; Moseev, T.; Chupakhin, O.; Charushin, V.; Trofimov, B. Metal-Free C–H Functionalization of 2H-Imidazole 1-Oxides with Pyrrolyl Fragments in the Design of Novel Azaheterocyclic Ensembles. *Org. Biomol. Chem.* **2017**, *15*, 8280–8284. [CrossRef] [PubMed]
44. Thompson, M.A. Molecular docking using ArgusLab, an efficient shape-based search algorithm and AScore scoring function. In Proceedings of the ACS Meeting, Philadelphia, PA, USA, 22–26 August 2004; p. 172.

45. Daina, A.; Michielin, O.; Zoete, V. SwissADME: A Free Web Tool to Evaluate Pharmacokinetics, Drug-Likeness and Medicinal Chemistry Friendliness of Small Molecules. *Sci. Rep.* **2017**, *7*, 42717. [CrossRef] [PubMed]
46. Gupta, M.; Lee, H.J.; Barden, C.J.; Weaver, D.F. The Blood–Brain Barrier (BBB) Score. *J. Med. Chem.* **2019**, *62*, 9824–9836. [CrossRef] [PubMed]